INTERNATIONAL SOCIETY FOR SOIL MECHANICS AND GEOTECHNICAL ENGINEERING

Numerical simulation of cone penetration testing using a unified state parameter model for clay and sand

Laurin Hauser

Graz University of Technology, Graz, Austria, laurin.hauser@tugraz.at

Helmut F. Schweiger

Graz University of Technology, Graz, Austria, helmut.schweiger@tugraz.at

ABSTRACT: Cone penetration testing (CPT) is a common in-situ investigation method where soil properties are derived from the measured quantities using correlations. Well-established correlations provide reliable results for clays and sands, where undrained or drained behavior governs the penetration process. However, the interpretation of CPT-data for intermediate soils, as they are typically found in Alpine basins in Austria, is difficult since partial drainage comes into play. In this work, the particle finite element method (G-PFEM) is used for the fully-coupled simulation of such a penetration problem in order to investigate partial drainage using the state parameter based Clay and Sand Model (CASM). The implementation of the constitutive model is presented and validated by means of a cavity expansion problem. Eventually, the approach allows to investigate the influence of different state boundary surfaces under changing drainage conditions on the measured CPTu quantities for Austrian silts.

Keywords: cone penetration testing, clay and sand model, partial drainage, Particle Finite Element Method

1. Introduction

In-situ investigation methods provide essential information on the characteristics of geomaterials in geotechnical engineering. The relevant mechanical parameters are generally derived using correlations based on various measured quantities. In cone penetration testing (CPTu), the tip resistance q_c, the sleeve friction f_s and the pore water pressure u_2 are continuously recorded while the probe is pushed into the soil at a constant rate of 2 cm/s. The probe has a conical tip with a base area of 10 or 15 cm².

A number of well-established correlations is available for the determination of the required soil properties. Most of them are based on either drained or undrained behavior during cone penetration as usually expected for sands or clays respectively. However, the application for silty soils is not straightforward due to the partially drained soil response.

Such postglacial silty deposits are also found in Alpine basins in Austria, like the region around Salzburg, where growing demand for construction projects represents a driving force for an improved characterization of the mentioned intermediate soils. Experience showed that conventional laboratory testing may provide misleading results for these sensitive deposits due to significant disturbance of the soil specimen during recovery and transportation. Therefore, in-situ investigation methods, such as CPTu, are a promising alternative and further understanding of the response of silty soils during testing is a key issue in order to improve and adapt correlations.

State-of-the-art numerical methods are capable of providing solutions to the problem of a cone penetrating a soil body while complex constitutive models take into account the non-linear soil behavior. The present work aims to present a numerical model for CPTu simulations based on the Particle Finite Element Method (PFEM) using the Clay and Sand Model (CASM). Thereby, the influence of the constitutive model with regards to the modelling of cone penetration in silty soils are highlighted.

2. Numerical model

The simulation of cone penetration is a complex task as large deformations, non-linear material behavior and frictional contact need to be considered as an ideally rigid cone penetrates a fully saturated soil body. Cone penetration has already been successfully modelled by means of different numerical methods, like the Arbitrary Eulerian-Lagrangian Method [1], the Material Point Method ([2], [3]) or the PFEM. In the scope of this work the application G-PFEM is used which is based on the latter approach ([4], [5]).

2.1. G-PFEM

The PFEM solves a given boundary value problem while performing a frequent remeshing of critical regions of the integration domain. At the beginning of a time step, the domain is treated as a cloud of particles/nodes that carry all information. Then, nodes may be added or removed depending on the nodal density, boundaries of the domain are defined, a new mesh is created and eventually the computation step is solved using the Finite Element Method (FEM). Consequently, an updated cloud of nodes is generated [6]. This strategy allows to deal with large deformations of the domain (avoiding excessive mesh distortion) but at the same time increases the computation time significantly. Therefore, linear triangular elements in connection with a stabilized and mixed formulation of the quasi-static linear momentum and mass balance equations in an updated Lagrangian setting are chosen where the determinant of the deformation gradient is introduced as a nodal variable additional to the displacement vector and the water pressure [7].

2.2. Clay and Sand Model

The state parameter based clay and sand model (CASM, [8]) is a non-associative, elastoplastic model formulated within the framework of critical state soil mechanics. The state parameter

$$\xi = v + \lambda \ln p' - \Gamma \qquad (1)$$

represents the difference in specific volume between the current stress state (v) and critical state (CS) at the same effective mean stress level which depends on the constants λ and Γ (see Fig. 1). At CS, ξ is equal to zero while $\xi > 0$ characterizes a looser state and $\xi < 0$ a denser state.
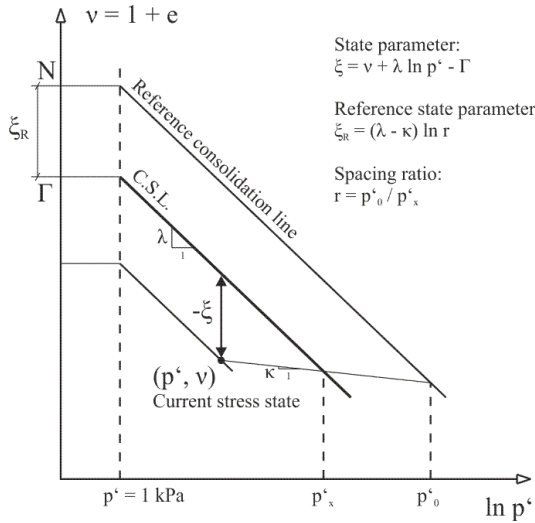
Figure 1. Representation of state parameter and critical state constants according to [8].

Furthermore, two additional material parameters, namely the spacing ratio r and the shape parameter n, are introduced to control the shape of the yield surface in the p'-q space with M being the slope of the CS-line and the preconsolidation pressure p'_0:

$$f = \left(\frac{q}{Mp'}\right)^n + \frac{1}{\ln r} \ln \frac{p'}{p'_0} \qquad (2)$$

Hence, the model is capable to capture the mechanical behavior of a wider range of geomaterials including intermediate, silty soils. At the same time, classical models like the Original Cam Clay Model (OCCM) or the Modified Cam Clay Model (MCCM) can be recovered for corresponding combinations of r and n as demonstrated in Fig. 2(a). The adopted plastic potential is an ellipse in the p'-q stress space (inspired by the yield surface of the MCCM) with a horizontal tangent at critical state.

Further, the CASM was adapted to finite strain theory according to the framework presented in [9]: In contrast to the additive decomposition of the small strain tensor $\boldsymbol{\varepsilon} = \boldsymbol{\varepsilon}_e + \boldsymbol{\varepsilon}_p$ the multiplicative split of the deformation gradient $\boldsymbol{F} = \boldsymbol{F}_e \cdot \boldsymbol{F}_p$ into an elastic and plastic part holds. The hyperelastic model of [10] yields the stress-strain-relation formulated in terms of Kirchhoff stresses $\boldsymbol{\tau}$ and the logarithmic Hencky strain tensor $\boldsymbol{\varepsilon}_h$. Consequently, the yield surface and the plastic potential depend on the invariants of $\boldsymbol{\tau}$ and the preconsolidation pressure p'_0

which evolves with plastic, volumetric stain. The explicit stress integration of the model in G-PFEM is based on [11]. Fig. 2(b) illustrates the stress paths of a constant volume direct shear test performed on the integration point for different combinations of r and n.

(a)

(b)
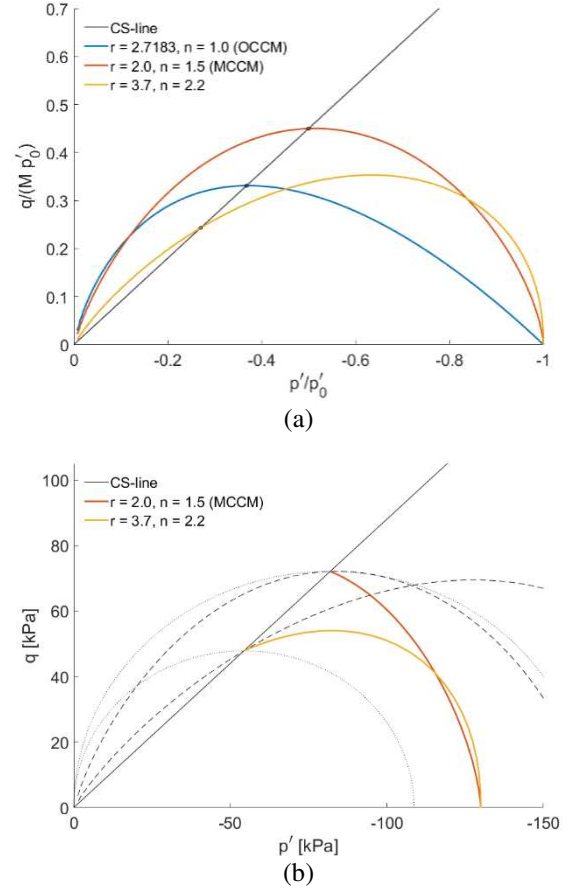
Figure 2. CASM yield surface in the normalized p'-q space (a) and stress paths of constant volume direct shear tests with yield surface (dashed line) and plastic potential (dotted line) at CS (b).

2.3. Undrained cavity expansion using CASM

An undrained spherical cavity expansion problem was recalculated using G-PFEM and the CASM and compared with the analytical solution in [12]. The axisymmetric model consists of (a quadrant of) an annulus whose inner radius a is expanded by prescribing radial displacements. The isotropic initial stress of 88 kPa acts as a line pressure on the outer boundary of the domain with the outer radius $A = 200 \, a_0$. Furthermore, a ratio between cavity expansion velocity and soil permeability of 10^{-9} m/s is chosen in order to ensure undrained conditions when using the coupled two-phase formulation. The material parameters are derived from [12] including the modified virgin consolidation and swelling slopes $\lambda^* = 0.076$ and $\kappa^* = 0.029$, the effective friction angle $\varphi' = 22.75°$, $p'_0 = 352$ kPa, an overconsolidation ratio of 4 and the CASM parameters $r = 2.7183$ and $n = 1$. However, the elastic parameters used for the analytical solution cannot be transferred directly to the hyperelastic model as its Poisson's ratio is generally depending on the stress level. Consequently, two different shear moduli G_0 (1000 and 1500 kPa) are used for the recalculation whereas the analytical solution is expected to lie between the two cases.
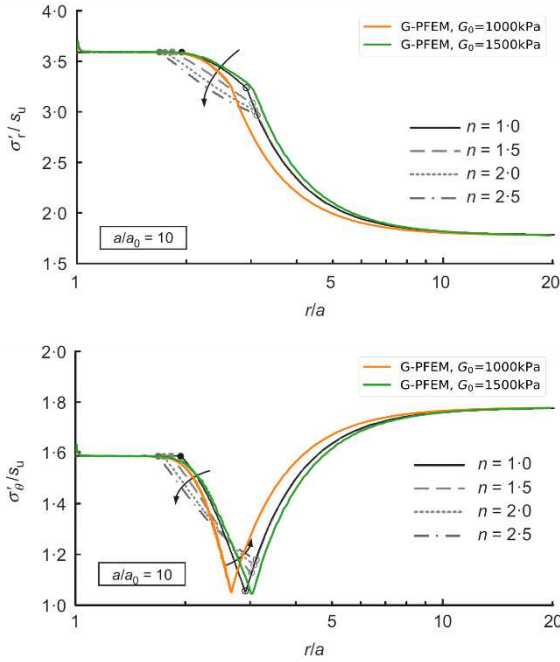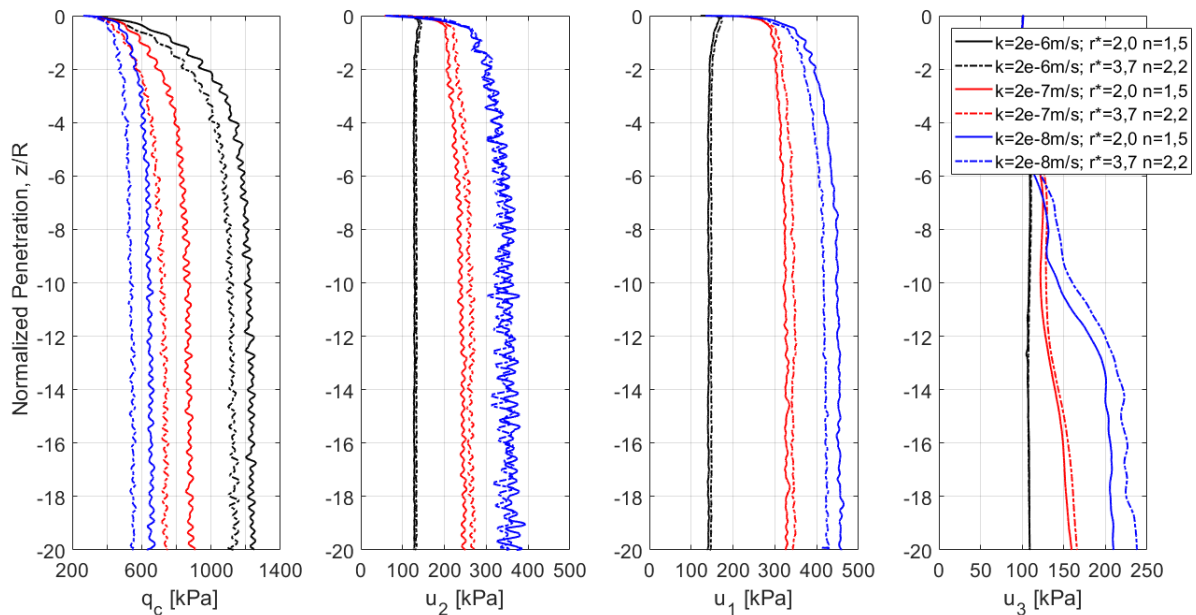
Figure 3. Comparison of numerical (G-PFEM) and analytical [12] results in terms of normalized effective radial (σ'_r/s_u) and circumferential (σ'_θ/s_u) stresses over normalized radius.

After expanding the cavity ($a/a_0 = 10$) the resulting spatial distributions of radial and circumferential effective stresses normalized with respect to the undrained shear strength s_u are compared and shown in Fig. 3. The numerical results show good overall agreement with the analytical solution. As expected, the latter is located between the numerical solutions indicating that G_0 influences the size of the plastic zone.

3. CPTu simulation

The validated CASM was further used for the simulation of cone penetration under partially drained conditions and the influence of the parameters r and n on the obtain CPTu quantities is investigated.

3.1. Model for cone penetration

The given insertion problem leads to an axisymmetric model including a rectangular, deformable soil body (height of 1.2 m and width of 0.5 m) and a rigid cone with a radius R of 1.78 cm and a tip angle of 60°. The latter is already inserted in the soil before the translatory movement (at 2 cm/s) along the symmetry axis is imposed. The total overburden pressure is specified on top of the domain while displacement in normal direction is fixed along the lateral and lower boundaries. Water drains freely along the outer boundaries except for the symmetry axis. The model and the initial mesh are shown in Fig. 4.
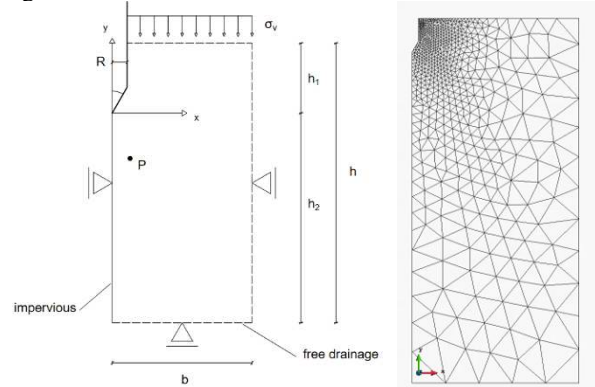
Figure 4. Axisymmetric model with the stationary measurement point P and the initial mesh.

The stiffness and strength parameters are based on [13] representing a layer of 'Salzburger Seeton' (the already mentioned postglacial silty deposit in the area of Salzburg) at a depth of around 12 to 13 m resulting in an initial isotropic effective stress of 130 kPa and an initial water pressure of 100 kPa. At this point, the simulations consider weightless soil and no friction along the cone interface. The basic input parameters are summarized in Table 1.

Figure 5. Calculated CPTu measurands over normalized depth z/R including the tip resistance q_c and the water pressures u_1, u_2, u_3 for different yield surface geometries ($r = 2/n = 1.5$ and $r = 3.7/n = 2.2$) under changing drainage conditions.

Table 1. Input parameter for 'Salzburger Seeton'.

γ [kN/m³]	λ* [-]	κ* [-]	φ' [°]
0	0.015	0.005	22.5

| G_0 [kPa]	α [-]	p'_0 [kPa]	OCR [-]
2900	0	130	1

3.2. CASM under partial drainage

Further, two parameter sets for r and n are introduced: The combination $r = 2$ and $n = 1.5$ approximates the MCC yield surface resulting in almost associated behaviour for the adopted plastic potential. Alternatively, non-associativity is obtained for $r = 3.7$ and $n = 2.2$. The latter combination was calibrated for a silty sand from Porto [14]. Fig. 5 shows the resulting penetration curves for the tip resistance q_c and the pore pressures u_1 to u_3 obtained for different r-n pairs and changing soil permeability ranging from $2*10^{-8}$ to $2*10^{-6}$ m/s. As expected, the basic trends, namely increasing tip resistance and decreasing pore pressures with increasing permeability, are evident for both cases. The highest considered permeablity of $2*10^{-6}$ m/s is already close to ideally drained conditions with equally low measured excess pore pressures for both combinations of r and n. As the soil gets less permeable the different yield surfaces result in different pore pressures at the three measurement positions. A permeability of $2*10^{-7}$ m/s results in slightly higher u_1, u_2 and u_3 pressures for $r = 3.7$ and $n = 2.2$ whereas the MCC approximation gives higher values for u_1 and u_2 for k = $2*10^{-8}$ m/s suggesting that the distribution of the generated water pressures around the cone is affected by the chosen yield surface geometry. The results also show that the combination of $r = 2$ and $n = 1.5$ leads to higher tip resistances for all drainage conditions.

3.3. Stress paths

Additionally, stress paths were analyzed for a fixed point P located at a depth of 0.3 m right next to the penetrating cone (see Fig. 4). Therefore, a stationary node at the given position is introduced during the remeshing in order to obtain the relevant data, which includes the nodal water pressure and the stresses taken from the neighbouring integration points.

Fig. 6 shows the effective stress paths and the evolution of the pore pressure during the penetration process until the shoulder of the cone is right next to P (at a depth of 0.331 m, $z/R = 18.6$). Qualitatively, the stress paths are very similar for both combinations of r and n: For the most permeable case p' and q increase significantly compared to the initial state. The stress path reaches CS and moves along the CSL due to stress redistribution. Undrained loading until CS is observable for $k = 2*10^{-8}$ m/s whereby the influence of the different yield surfaces is clearly outlined. It should be noted that the unsteady jumps at the end of each stress path may also be significantly influenced by the closeby cone shoulder, the most problematic geometric feature. However, the moblized shear strength for $r = 3.7$ and $n = 2.2$ is lower explaining the observed lower tip resistance. The stress paths for $k = 2*10^{-7}$ m/s consist of a clear undrained initial loading phase followed by a simultaneous increase of p'

and q similar to the path for $2*10^{-6}$ m/s. This can also be seen by means of the identical pore pressure evolutions until reaching the normalized depth of $z/R = 12$. Also, the position of the peak pressures with respect to the normalized penetration depth suggest that the shape of the generated excess pore pressure bulb strongly depends on the soil permeability.
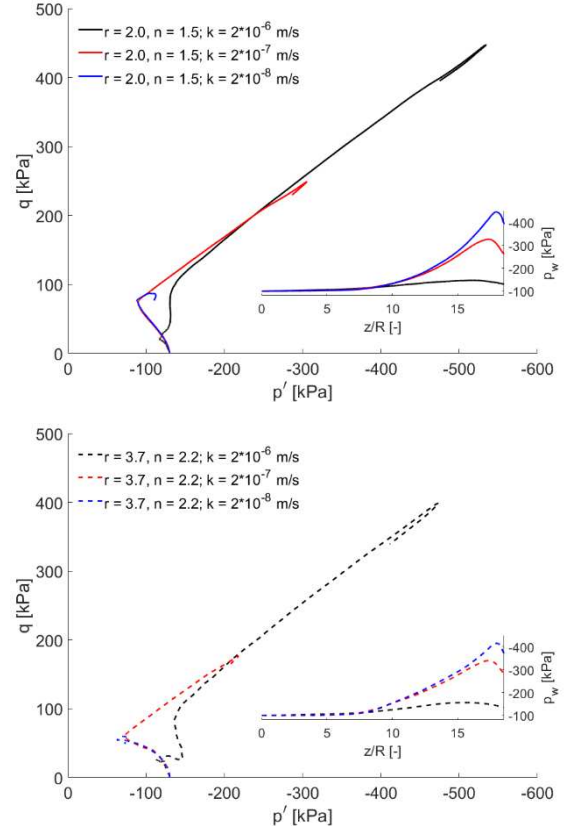
Figure 6. Effective stress paths in the p'-q plot and pore pressure evolution at measurement point P after 0.331 m of penetration ($z/R = 18.6$) for different r-n combinations and permeabilities.

4. Conclusion

The CASM allows to model a wide range of soils due to the flexible definition of the yield surface combined with a non-associated flow rule. It was shown that the model can be successfully used for the numerical simulation of cone penetration within the G-PFEM framework highlighting the influence of the model parameters r and n. Thus, it is believed that the approach is a valuable contribution to understanding the behaviour of silty soils during cone penetration. Future work includes the calibration of the numerical model based on in-situ and laboratory data for Austrian postglacial silty deposits. Furthermore, the CASM may also be extended in order to account for structure and bonding according to the framework presented in [15].

References

[1] Sheng, D., Kelly, R., Pineda, J., Lachlan, B. "Numerical study of rate effects in cone penetration test", In: 3rd International Symposium on Cone Penetration Testing, Las Vegas, Nevada, USA, 2014, pp. 419-428.

[2] Beuth, L. "Formulation and Application of a Quasi-Static Material Point Method", PhD Thesis, Universität Stuttgart, 2012.

[3] Ceccato, F., Simonini, P. "Numerical study of partially drained penetration and pore pressure dissipation in piezocone test", Acta

Geotechnica, 12(1), pp. 195-209, 2017. https://doi.org/10.1007/s11440-016-0448-6

[4] Monforte, L., Arroyo, M., Carbonell, J.M., Gens, A. "Numerical simulation of undrained insertion problems in geotechnical engineering with the Particle Finite Element Method (PFEM)", Computers and Geotechnics 82, pp. 144-156, 2017. https://doi.org/10.1016/j.compgeo.2016.08.013

[5] Monforte, L., Arroyo, M., Carbonell, J.M., Gens, A. "Coupled effective stress analysis of insertion problems in geotechnics with the Particle Finite Element Method", Computers and Geotechnics 101, pp. 114-129, 2018. https://doi.org/10.1016/j.compgeo.2018.04.002

[6] Oñate, E., Idelsohn, S.R., Celigueta, M.A., Rossi, R., Marti, J., Carbonell, J.M., Ryzakov, R., Suárez, B. "Advances in the Particle Finite Element Method (PFEM) for Solving Coupled Problems in Engineering", In: Oñate E., Owen D.R.J. (eds.) Particle-Based Methods. Computational Methods in Applied Sciences, vol 25. Springer, Dordrecht, The Netherlands, 2011, pp. 1-49. https://doi.org/10.1007/978-94-007-0735-1_1

[7] Monforte, L., Carbonell, J.M., Arroyo, M., Gens, A. "Performance of mixed formulations for the particle finite element method in soil mechanics problems", Computational Particle Mechanics 4(3), pp. 269-284, 2017. https://doi.org/10.1007/s40571-016-0145-0

[8] Yu, H.S. "CASM: a unified state parameter model for clay and sand", International Journal for Numerical and Analytical Methods in Geomechanics 22, pp. 621-653, 1998. https://doi.org/10.1002/(SICI)1096-9853(199808)22:8<621::AID-NAG937>3.0.CO;2-8

[9] Monforte, L., Arroyo, M., Gens, A., Carbonell, J.M. "Integration of elasto-plastic constitutive models in finite deformation: An explicit approach", In Oñate E., Owen D.R.J., Peric, D., Chiumenti, M. (eds.) Proceedings of the XIII International Conference on Computational Plasticity, Barcelona, Spain, 2015, pp. 398-406.

[10] Houlsby, G.T. "The use of a variable shear modulus in elastic-plastic models for clays" Computers and Geotechnics 1(1), pp. 3-13, 1985. https://doi.org/10.1016/0266-352X(85)90012-6

[11] Sloan, S.W., Abbo, A.J., Sheng, D. "Refined explicit integration of elastoplastic models with automatic error control", Engineering Computations 18, pp. 121-154, 2001. https://doi.org/10.1108/02644400110365842

[12] Mo, P.Q., Yu, H.S. "Undrained cavity expansion analysis with the unified state parameter model for clay and sand", Géotechnique 67(6), pp. 503-515, 2017. https://doi.org/10.1680/jgeot.15.P.261

[13] Sachsenhofer, M. "Comparison of correlations from CPTu, SDT, DP", Master's Thesis, Graz University of Technology, 2012.

[14] Rios, S., Cianta, M., Gonzalez, N., Arroyo, M., da Fonseca, A.V. "Simplifying calibration of bonded elasto-plastic models", Computers and Geotechnics 73, pp. 100-108, 2016. https://doi.org/10.1016/j.compgeo.2015.11.019

[15] Gens, A., Nova, R. "Conceptual bases for a constitutive model for bonded soils and weak rocks", In: Anagnostopoulos, A. (ed.) Geotechnical engineering of hard soils – soft rocks. International symposium: Papers, vol 1-3. A A Balkema, Rotterdam, Brookfield, USA, 1993, pp. 577-583.